THE COMPUTATION OF POLEFACE WINDING SYSTEMS YIELDING INDEPENDENT MULTIPOLE FIELDS WITHIN THE APERTURE OF NOTABLY ALTERNATING GRADIENT SYNCHROTRON MAGNETS

A. Asner, R. Holsinger and Ch. Iselin

Introduction and Summary

The 28 GeV Proton Synchrotron of CERN (CPS) is now 15 years old. Initially planned as an accelerator for 25 GeV physics, the CPS is developing into the key element of an accelerator complex comprising recently built machines such as the 28 GeV Intersecting Storage Rings (ISR), the 800 MeV PS Booster (PSB), and the 300 GeV SPS now under construction.

The CPS should thus accomplish a fourfold task: to accept from the PSB a high-intensity beam of 4-5 × 10^{12} p/pulse -- to be increased later to 10^{13} p/pulse; to accelerate and to distribute this beam to the ISR and the 25 GeV physics experimental areas; and to serve from 1976 onward as a reliable high-intensity 10 GeV injector for the SPS.

In order to perform these tasks with success, a number of complex injection and slow and fast extraction systems have been developed which occupy a considerable part of the straight sections. In return, many initially mounted correcting lenses have had to be withdrawn from these straight sections.

The problem of poleface windings (PFW) is intimately related to a successful future high-intensity injection and acceleration in the CPS. The PFW system has initially been foreseen to compensate remanent field and vacuum chamber eddy current effects at injection and to provide a certain compensation at saturation, i.e. a limited good field region at medium intensities when increasing the energy up to 28 GeV.

Recent investigations of the status of the actual PFW's revealed the following:

i) The now 15 year-old components and impregnation of the PFW do not meet today's radiation resistance requirements, even at present intensities of 1.5-2 × 10^{12} p/pulse. Replacement of the most irradiated PFW units will continue until 1975, when a general replacement of the entire PFW system will have to be envisaged.

ii) The future complex CPS operation implies full control of the working point at injection, during acceleration, and at extraction. Chromaticity of the entire aperture and not only of the beam central part should be under control and collective instability phenomena controlled and compensated.

In addition to injection and saturation error compensation one would aim at a PFW system allowing independent adjustment of Q_H and Q_V and of their first-second- $[\partial Q_{H(V)}/\partial\rho,\ \partial^2 Q_{H(V)}/\partial\rho^2]$, and perhaps higher-order derivatives. Compensation of high-intensity beam instabilities requires sextupole and octupole fields; higher-multipole fields could be useful for straightening the Q_H-Q_V curves at high-intensity acceleration.

An adequate PFW system should thus be capable of creating independent quadrupole, sextupole, octupole, and higher-order fields, or any of their linear combination.

In this paper we present the computations for such a system which would consist of n conductors along the pole contour, supplied from n + 1 separate power supplies. By varying the currents in the n conductors and the return current balance, a very convenient practical layout can be obtained.

We have succeeded in approximating the required theoretical line current distribution along the pole by only 4 or 5 discrete conductors carrying optimized currents and yielding the required multipoles: a $\partial B/\partial\rho$ = 0.4 Tm^{-1} quadrupole, $\partial^2 B/\partial\rho^2$ = 12 Tm^{-1} sextupole, and $\partial^3 B/\partial\rho^3$ = 70 Tm^{-3} octupole. The multipole field errors could, within ±5 cm, be reduced to $\Delta B_n \leq \pm 0.3$ G.

The highest single conductor current for compensation of saturation at 28 GeV plus the highest sextupole and octupole correcting multipoles would amount to ≈ 2 kA.

Computation of PFW systems yielding harmonic multipole fields within the aperture of combined function accelerator magnets

The method consists in finding the multipole field tangential component B_t (T) along the pole contour and expressing its proportionality with the line current density j_ℓ (Am^{-1}):

$$B_t = j_\ell \cdot \mu_0 \tag{1}$$

Expressions will now be derived for the line current density j_ℓ and for the line currents along the incremental contour length Δs - $I_\ell = j_\ell \cdot \Delta s$ as well as for the horizontal projection $I_{h_{\Delta x}}$ -- such as to yield multipole fields of the type:

$$B = B_x + iB_y = \frac{\partial^n B}{\partial\rho^n} \cdot \frac{1}{n!} (x - iy)^n \ . \tag{2}$$

The pole contour may be a hyperbola or part of a circle or straight line:

$$y = \frac{c}{(x + a)} \tag{3}$$

$$y = y_0 + \sqrt{r^2 - (x - x_0)^2} \tag{4}$$

$$y = kx \ . \tag{5}$$

Hyperbolic pole profile

In accordance with Fig. 1 one obtains for a dipole field B_0:

$$B_t = B_0 \sin\alpha = - \frac{B_0 y}{\sqrt{y^2 + (x + a)^2}} \tag{6}$$

$$I_\ell = - \frac{B_0 y \cdot \Delta s}{\mu_0 \sqrt{y^2 + (x + a)^2}} \tag{7}$$

and for the more interesting current I_h corresponding to the horizontal projection of I_ℓ:

$$I_h = - \frac{B_0\ \Delta x\ c}{\mu_0 (x + a)^2} \ . \tag{8}$$

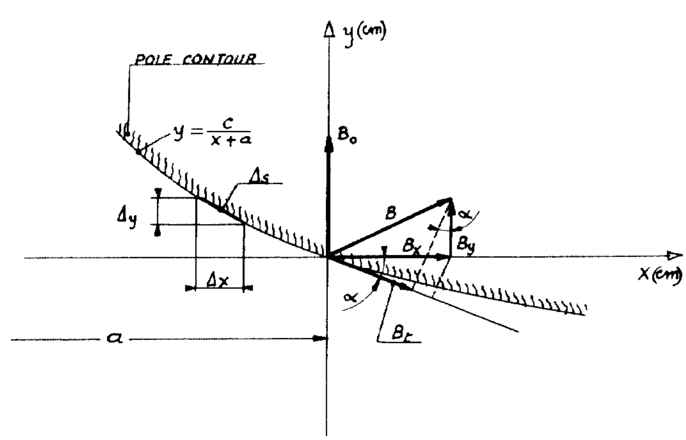

Fig. 1

For a quadrupole field with the gradient G (Tm^{-1}) one has in accordance with Fig. 1:

$$B_t = B_x \cos \alpha + B_y \sin \alpha = G \left[\frac{y(x + a)^2 - cx}{\sqrt{(x + a)^4 + c^2}}\right] \quad (9)$$

and

$$I_h = \frac{\Delta x \; G \; ca}{\mu_0 (x + a)^2} \; . \quad (10)$$

The expressions for I_h yielding a sextupole, octupole, and decapole field are:

$$I_h = \frac{(\partial^2 B/\partial\rho^2)\Delta xc}{2\mu_0}\left[\frac{(x^2 + 2ax)(a + x)^2 + c^2}{(x + a)^4}\right] . \quad (11)$$

For an octupole and decapole field one has

$$I_h = \frac{(\partial^3 B/\partial\rho^3)\Delta x}{6\mu_0}\left[\frac{3x^2c - cy^2 - x^3y + 3xy^3}{x + a}\right] \quad (12)$$

and

$$I_h = \frac{(\partial^4 B/\partial\rho^4)\Delta x}{24\mu_0}\left[\frac{(x + a)^5 \cdot 4x^3c - (x + a)^3 \; 4xc^3}{(x + a)^6} - \right.$$

$$\left. - \frac{(x + a)^4 \; cx^4 + (x + a)^2 \; 6x^2c^3 - c^5}{(x + a)^6}\right] . \quad (13)$$

Circular profile part

Equations 14 to 18 give I_h for dipole, quadrupole, sextupole, octupole, and decapole field configurations:

$$I_h = - \frac{\Delta x B_0}{\mu_0} \cdot \frac{y - y_0}{x - x_0} \quad (14)$$

$$I_h = \frac{\Delta x(\partial B/\partial\rho)}{\mu_0}\left[y - x \frac{y - y_0}{x - x_0}\right] \quad (15)$$

$$I_h = \frac{\Delta x(\partial^2 B/\partial\rho^2)}{2\mu_0}\left[2xy - (x^2 - y^2) \cdot \frac{y - y_0}{x - x_0}\right] \quad (16)$$

$$I_h = \frac{\Delta x(\partial^3 B/\partial\rho^3)}{6\mu_0}\left[3x^2y - y^3 - (x^3 - 3xy^2) \cdot \frac{y - y_0}{x - x_0}\right] \quad (17)$$

and

$$I_h = \frac{\Delta x(\partial^4 B/\partial\rho^4)}{24\mu_0}\left[4xy(x^2 - y^2) - \right.$$

$$\left. - (x^4 - 6x^2y^2 + y^4) \frac{y - y_0}{x - x_0}\right] . \quad (18)$$

Straight-line profile part

The corresponding expressions for I_h are given below:

$$I_h = \Delta x \cdot B_0 \cdot k \; | \; \mu_0 \quad (19)$$

$$I_h = \frac{2\Delta x(\partial B/\partial\rho)}{\mu_0} \cdot kx \quad (20)$$

$$I_h = \frac{\Delta x(\partial^2 B/\partial\rho^2)}{2\mu_0}\left[2xy + k(x^2 - y^2)\right] \quad (21)$$

$$I_h = \frac{\Delta x(\partial^3 B/\partial\rho^3)}{6\mu_0}\left[3x^2y - y^3 + k(x^3 - 3xy^2)\right] \quad (22)$$

$$I_h = \frac{\Delta x(\partial^4 B/\partial\rho^4)}{24\mu_0}\left[4xy(x^2 - y^2) + k(x^4 - 6x^2y^2 + y^4)\right] . \quad (23)$$

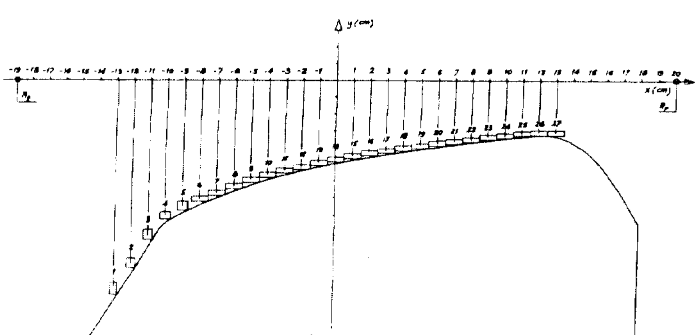

Fig. 2

Table 1

Conductor No.	I (A)	Conductor No.	I (A)
1	920	14	195
2	775	15	184
3	663	16	170
4	570	17	158
5	500	18	147
6	442	19	137
7	393	20	128
8	350	21	120
9	315	22	113
10	285	23	106
11	260	24	100
12	236	25	94.5
13	216	26	89
		27	84.6

It should be noted that the multipole field expansion according to Eq. (2) is strictly valid within a circle of radius r equal to the half gap height at equilibrium orbit. In the CPS the corresponding radius is r = 5 cm.

To check the validity of the exposed method, the current distribution for a quadrupole field of 0.49 Tm^{-1} has in accordance with Fig. 2 been approximated by 27 rectangular 30 mm^2 conductors along the CPS pole contour. The corresponding currents are given in Table 1. The current pattern with the two return currents on the horizontal axis has been checked by the computer program MAGNET of Ch. Iselin; the result was a 0.48 ± 0.02 Tm^{-1} field gradient within -8 cm < x < 8 cm.

Possible practical solutions: optimized 4-5 conductor PFW systems yielding the required saturation compensation and the correcting quadrupole, sextupole, and octupole multipoles

The quantitative requirements to be met by a new CPS PFW system can be summarized as follows:

i) Compensation of saturation up to the highest energy of 28 GeV, corresponding to a main 1.42 T magnetic field on the equilibrium orbit.

From Fig. 3, showing the measured n = n(x) curve for the CPS magnet, one can express the saturation effect within -5 cm < x < 5 cm as:

$$\text{Saturation} = 0.4 \; Tm^{-1} + 6 \; Tm^{-2} + 25 \; Tm^{-3} + \ldots \; . \quad (24)$$

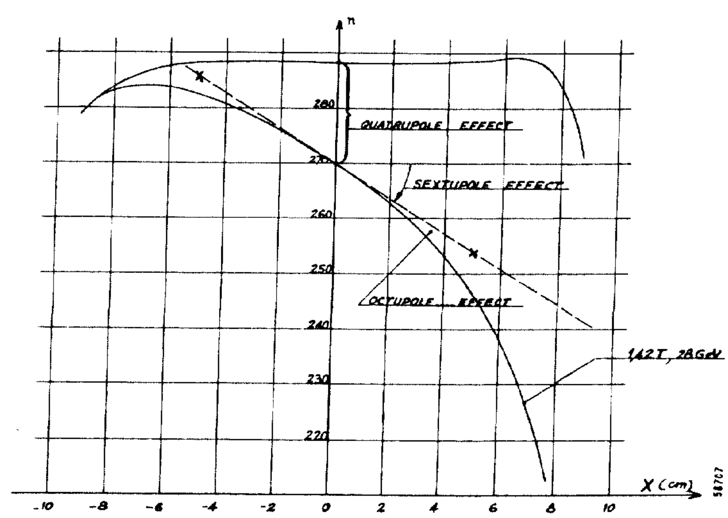

Fig. 3

The PFW system should also be capable of:

ii) providing a $\partial B/\partial\rho = 0.38 \pm 0.02\ \mathrm{Tm^{-1}}$ quadrupole for ΔQ shift;

iii) providing an additional $\partial^2 B/\partial\rho^2 = \pm 4\ \mathrm{Tm^{-2}}$ sextupole for chromaticity regulation, and

iv) an additional octupole $\partial^3 B/\partial\rho^3 = 45\ \mathrm{Tm^{-3}}$ for instability damping.

If possible, higher-order multipoles should also be produced.

It is clear that PFW configurations such as the one shown in Fig. 2 have to be discarded in view of the prohibitive costs and problems of operation that the large number of power supplies would entail.

However, using the optimization computer program MIRT [1] developed by K. Halbach, which determines the individual conductor currents for a given field pattern within an aperture and minimizes the remaining field errors, and applying the reasoning by the same author,[1] we arrived at elegant solutions consisting of only 4 or 5 conductors per pole contour, still respecting the rather stringent requirements (i) to (iv).

The solution to the problem of selecting the number of conductors and the corresponding spacing between them was facilitated by examining Fig. 4, showing the field patterns produced by five individual conductors, fed by "unit currents" of 100 A. The left-hand return conductor R_ℓ effect is also shown (the right-hand conductor R_r, screened by the pole, does not contribute to the field pattern). The required saturation compensation, quadrupole, sextupole, and octupole fields should be produced by optimized superposition of the individual conductor field patterns.

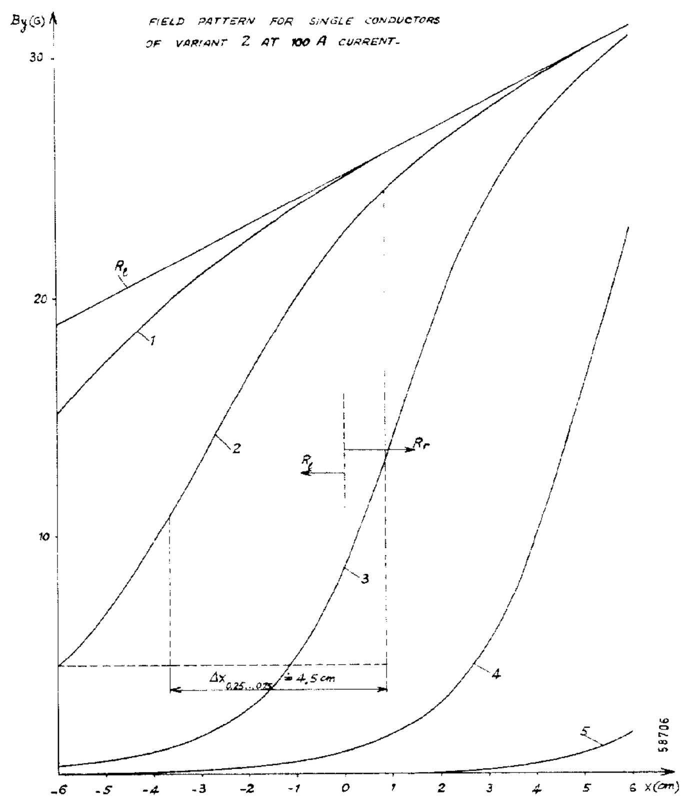

Fig. 4

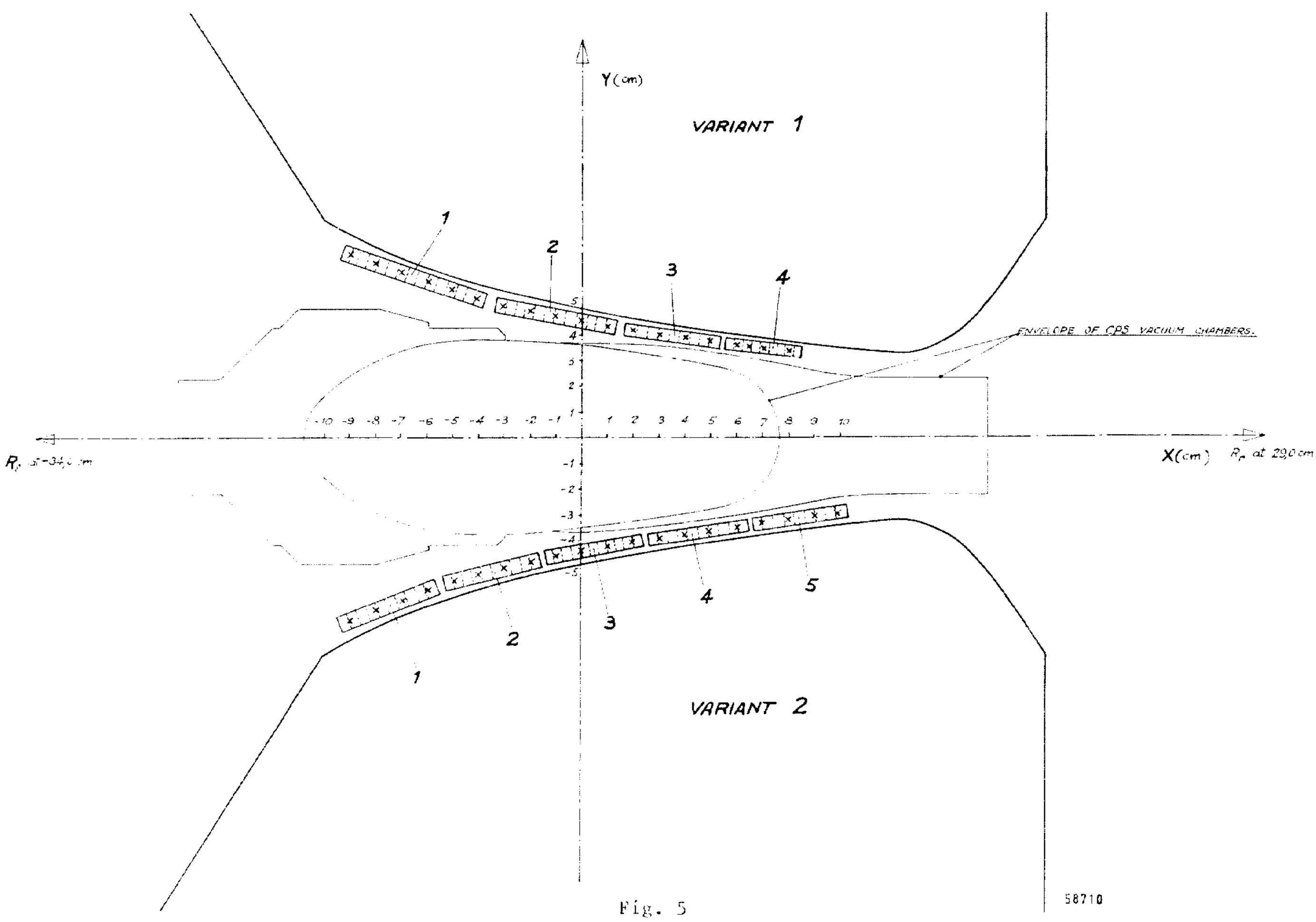

Fig. 5

Table 2

Four conductor variant parameters

Correcting multipole / Conductor	Quadrupole 0.4 (Tm^{-1}) I (A)	Sextupole 12 (Tm^{-2}) I (A)	Octupole 70 (Tm^{-3}) I (A)	Saturation I (A)	Saturation ±4 (Tm^{-2}) I (A)	Saturation ±4 (Tm^{-2}) + 45 (Tm^{-3}) I (A)	Saturation +45 (Tm^{-3}) I (A)
1	2156	-3522.0	434.0	550.0	1724.0	2003.0	828.0
2	790	84.9	-90.7	799.9	828.2	769.9	741.6
3	494.8	576.6	44.6	799.1	991.2	1019.9	827.8
4	278.1	932.1	183.8	809.9	1120.6	1238.8	928.1
Return balance	41.9	-136.8	-25.2	164.5	210.1	193.9	148.3

Table 3

Five conductor variant parameters

Correcting multipole / Conductor	Quadrupole 0.4 (Tm^{-1}) I (A)	Sextupole 12 (Tm^{-2}) I (A)	Octupole 70 (Tm^{-3}) I (A)	Saturation I (A)	Saturation ±4 (Tm^{-2}) I (A)	Saturation ±4 (Tm^{-2}) + 45 (Tm^{-3}) I (A)	Saturation +45 (Tm^{-3}) I (A)
1	2074.4	-4133.0	810.7	305.3	1683.0	2204.2	826.5
2	804.8	-489.7	-85.9	526.6	689.8	634.6	471.4
3	600.0	195.7	-30.3	687.3	752.5	733.0	667.8
4	446.4	728.2	57.6	831.0	1073.7	1110.8	868.1
5	371.6	1130.7	368.0	1069.0	1445.9	1682.5	1305.6
Return balance	381.5	-239.3	-19.0	352.9	432.1	420.5	340.7

Each individual field pattern can be characterized by its half-width between approximately the 0.25 and 0.75 amplitude points.

The number of individual conductors is related to this width and to the choice of field pattern spacing and overlapping. We have chosen conductor spacings of 4-6 cm, corresponding to the field pattern half-width in Fig. 4. The field patterns thus overlap sufficiently to produce the desired field and are not so close together to have nearly redundant effects.

Another important feature is the freely variable pole excitation or free repartition of the total return current between R_ℓ and R_r. This allows the optimized superposition of a dipole and quadrupole field (from the hyperbolic pole shape) upon the fields from the PFW conductors. The total PFW field can, by this additional degree of freedom, be made to correspond more closely and with less current to the desired field configurations.

Expressed in other words, this additional degree of freedom can, in extremis, allow the current in any conductor to return either to the right or left conductors R_ℓ or R_r.

Figure 5 shows the two PFW variants with four conductors (upper part) and five conductors (lower parts).

Variant 1 would consist of only four conductors along the pole contour the cross-sections being 58 × 6 mm^2, 46 × 6 mm^2, 37 × 4.5 mm^2, and 30 × 4.5 mm^2, respectively.

Variant 2 would consist of five conductors of 40 × 6 mm^2 and 40 × 4.5 mm^2.

Care has been taken to locate the conductors with adequate insulation outside the envelope of the different CPS vacuum chambers.

Tables 2 and 3 summarize the main parameters for the proposed variants 1 and 2.

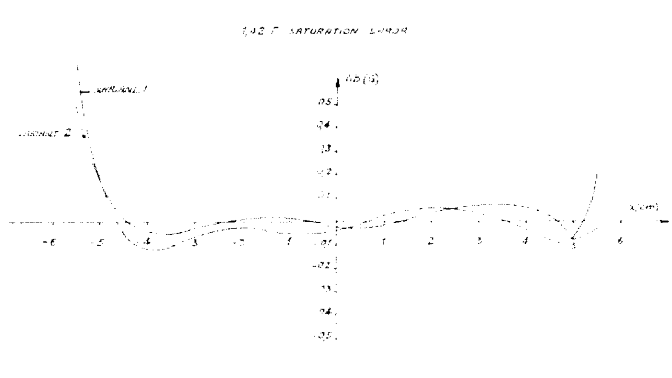

Fig. 6

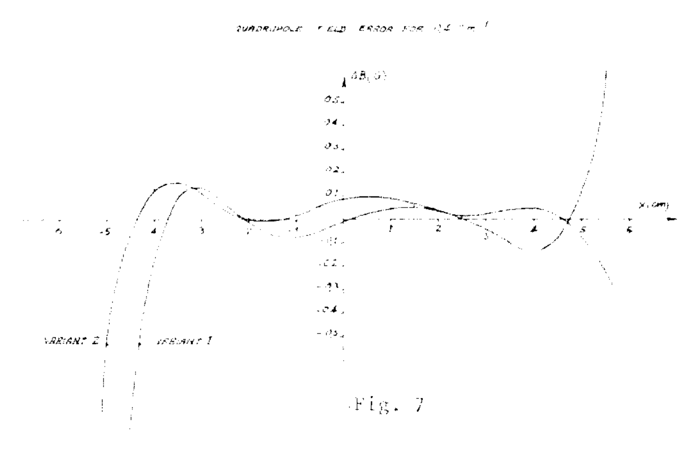

Fig. 7

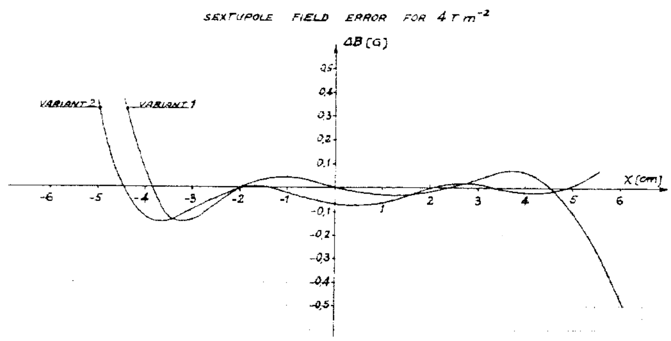

Fig. 8

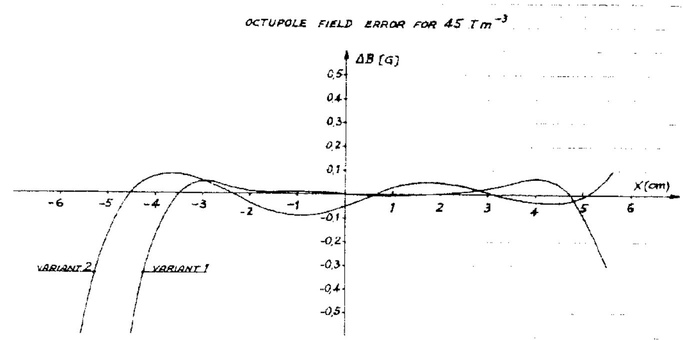

Fig. 9

Figures 6 to 9 show the remaining field errors on the midplane for the case of saturation compensation, quadrupole, sextupole, and octupole fields, as obtained by the computer program MIRT.

Since every conductor in Fig. 5 has been simulated by 3 to 6 point sources of equal current, the results are closely reflecting the true case of finite size conductors.

Annex I
Computation of the CPS magnet pole contour length Δs

Assuming an ideal hyperbolic profile given by Eq. (3), one can write:

$$ds = dx\,\sqrt{1 + y'^2} = dx\,\sqrt{1 + \frac{c^2}{(x + a)^4}}\ . \qquad (A.1)$$

Substituting

$$\frac{c}{(x + a)^2} = \mathrm{tg}\,\alpha \qquad (A.2)$$

one obtains

$$\Delta s_{x_1 \ldots x_2} = -\frac{\sqrt{c}}{2}\int_{x_1}^{x_2} \frac{(1 + \mathrm{tg}^2\,\alpha)^{3/2}}{(\mathrm{tg}\,\alpha)^{3/2}} \cdot d\alpha = -\sqrt{2c}\int_{x_1}^{x_2} \frac{d\alpha}{(\sin 2\alpha)^{3/2}}\ . \qquad (A.3)$$

The substitution $\sqrt{\sin 2\alpha} = t$ yields

$$\Delta s_{x_1 \ldots x_2} = -\sqrt{2c}\int_{x_1}^{x_2} \frac{dt}{t^2\sqrt{1 - t^4}}\ . \qquad (A.4)$$

A further substitution $1 - t^2 = v^2$ yields

$$\Delta s_{x_1 \ldots x_2} = \int_{x_1}^{x_2} \sqrt{2c}\,\frac{dv}{(1 - v^2)\sqrt{(1 - v^2)(2 - v^2)}}\ . \qquad (A.5)$$

The solution of Eq. (A.5) is the following combination of elliptic integrals:

$$\Delta s_{x_1 \ldots x_2} = \sqrt{c}\,\Big|_{x_1}^{x_2} \sqrt{1 - 0.5\,\sin^2\alpha} \cdot \mathrm{tg}\,\phi + 0.5 \cdot F(\phi,K) - E(\phi,K)\,\Big|_{x_1}^{x_2} \qquad (A.6)$$

with

$$\cos\phi = t = \sqrt{\sin 2\left[\mathrm{arctg}\,\frac{c}{(x + a)^2}\right]} \qquad (A.7)$$

and $K = 1/\sqrt{2}$, i.e. 45°.

$F(\phi,K)$ and $E(\phi,K)$ are elliptic integrals of the first and second kind, to be found in Jahnke and Emde.[2] It is, of course, simpler to compute the incremental pole contour length from:

$$\Delta s \approx \sqrt{(x_2 - x_1)^2 + (y_2 - y_1)^2} \qquad (A.8)$$

Acknowledgements

Helpful and critical discussions and remarks by Messrs K.H. Lohmann and P. Lefèvre, PS Department of CERN, are acknowledged.

References

1) A program for inversion of system analysis and its application to the design of magnets, UCRL report, July 1967.

2) Jahnke-Emde-Losch, Tables of higher functions (B.G. Trübner Verlag, Stuttgart, 1970).